

Climate Security Vulnerability in Africa Mapping 3.0

by

Joshua Busby
busbj@utexas.edu

Todd G. Smith
toddgsmith@utexas.edu

Nisha Krishnan
nisha.krishnan1@gmail.com

Mesfin Bekalo
mesfin@austin.utexas.edu

Strauss Center for International Security and Law
LBJ School of Public Affairs
University of Texas-Austin

Paper prepared for presentation at the 2013 Annual Meeting of the
International Studies Association
San Francisco, California, April 3-6, 2013

This material is based upon work supported by, or in part by, the U.S. Army Research Office contract/grant number W911NF-09-1-0077 under the Minerva Initiative of the U.S. Department of Defense.

Climate Security Vulnerability in Africa Mapping 3.0

Joshua Busby, Todd G. Smith, Nisha Krishnan, and Mesfin Bekalo

Climate change is expected to have severe consequences on the lives and livelihoods of millions of people around the world, but its effects will not be evenly distributed. As a result of accidents of geography, different locations face distinct sources of vulnerability based on their different exposure to cyclones, storm surge, drought, intense rains, wildfires, and other physical phenomena. The exposure of human populations to such physical processes varies, with large numbers of people often concentrated along the coasts while other areas are much less densely populated. Whether these populations are able to protect themselves from the worst consequences of exposure to climate related hazards is contingent upon other aspects, including their health status, level of education, and access to services. In many instances, even communities with high living standards and adequate access to information and services will find themselves tested by extreme events; how well they fare will be contingent on the willingness and ability of their governments to come to their aid in times of need.

In this context of multi-layered sources of climate vulnerability, the continent of Africa is thought to be among if not the most vulnerable location, given both high exposure to climate change and relatively low community resilience and governance capabilities.¹ However, even within Africa, vulnerability is not equally distributed.

¹ M. Boko et al., “Africa,” in *Climate Change 2007: Impacts, Adaptation and Vulnerability. Contribution of Working Group II to the Fourth Assessment Report of the Intergovernmental Panel on Climate Change*, ed. M.L. Parry et al. (Cambridge UK: Cambridge University Press, 2007), 433–467; IPCC, “Fourth Assessment Report -- Chapter 9: Africa,” 2007, <http://www.unep.org/pdf/ipcc/Ch09.pdf>; Reid Basher and Sálvano Briceño, “Climate and Disaster Risk Reduction in Africa,” in *Climate Change and Africa*, ed. Pak Sum Low (Cambridge: Cambridge University Press, 2005), 269–281.

With climate change adaptation looming ever larger as an important policy area, decisions have to be made about where to concentrate resources, both from national sources as well as international ones. Understanding where climate vulnerabilities are located therefore has immense practical significance.²

Four years ago, as part of the Department of Defense-funded Minerva Initiative, we initiated a mapping project to identify sub-national locations of what we came to call “climate security” vulnerability in Africa. Our intent was to go beyond mere livelihoods-based analyses of vulnerability to identify the places where the worst consequences of climate change were likely to hit and put large numbers of people at risk of mass death. Such situations had become humanitarian emergencies that required the mobilization of emergency resources by affected governments and donors alike, sometimes involving military mobilization by both or either to keep people from dying. Such situations may or may not escalate into incidences of armed conflict.

Over the past several years, we have published versions of those maps in a variety of outlets, beginning with in-house working papers and policy briefs at our host institution the Strauss Center for International Security and Law at the University of Texas.³ We then published a series of papers and articles in journals

² Lisa Friedman, “Which Nations Are Most Vulnerable to Climate Change? The Daunting Politics of Choosing,” 2010, <http://www.nytimes.com/cwire/2011/02/24/24climatewire-which-nations-are-most-vulnerable-to-climate-95690.html?ref=energy-environment>.

³ Joshua Busby et al., *Locating Climate Insecurity: Where Are the Most Vulnerable Places in Africa?* (Austin, Texas: Strauss Center for International Security and Law, 2010), http://ccaps.strausscenter.org/system/research_items/pdfs/19/original.pdf?1283195613; Joshua Busby, Kaiba White, and Todd G. Smith, *Locating Climate Insecurity: Where Are the Most Vulnerable Places in Africa* (Austin: Strauss Center for International Security and Law, 2011), <http://strauusscenter.org/ccaps/publications/research-briefs.html?download=97>.

and edited volumes,⁴ culminating in an article in the Spring 2013 issue of *International Security*.⁵ This current paper represents a major revision in our underlying modeling process, what we are calling the 3.0 version of our Climate Security Vulnerability Model (hereafter CSVM 3.0).⁶ This paper details the methodological refinements we have made to our model and the rationale for them, our findings, and closes with extensions for future research.

Part I: Mapping Climate Security Vulnerability

The aim of our maps remains consistent, even if our methods and approaches have evolved.⁷ Our goal is to identify the places most likely vulnerable to climate security concerns within Africa and go beyond national level vulnerability rankings to identify vulnerabilities at the sub-national level.

⁴ Joshua Busby et al., “Locating Climate Insecurity: Where Are the Most Vulnerable Places in Africa?,” in *Climate Change, Human Security and Violent Conflict*, ed. Jurgen Scheffran et al., Hexagon Series on Human and Environmental Security and Peace, 8 (Springer, 2012), 463–512; Joshua W. Busby, Todd G. Smith, and Kaiba White, “Climate Security and East Africa: A GIS-Based Analysis of Vulnerability,” in *Climate Change, Pastoral Traditional Coping Mechanisms and Conflict in the Horn of Africa*, ed. Gebre Hiwot Mulugeta and Jean-Bosco Butera (Addis Ababa: UPEACE, 2012); Joshua W. Busby, Kaiba White, and Todd G. Smith, “Mapping Climate Change and Security in North Africa,” *German Marshall Fund of the United States*, 2010, <http://www.gmfus.org/archives/mapping-climate-change-and-security-in-north-africa-full-text/>.

⁵ See Joshua W. Busby et al., “Climate Change and Insecurity: Mapping Vulnerability in Africa,” *International Security* 37, no. 4 (2013).

⁶ We also supervised a series of student working papers to test alternative formulations on a regional basis of our vulnerability model. Emily Joiner, Derell Kennedo, and Jesse Sampson, *Vulnerability to Climate Change in West Africa* (Austin, Texas: Strauss Center for International Security and Law, March 2012), <http://strausscenter.org/ccaps/climate-vulnerability-publications.html?download=55>; Sachin Shah, Sarah Williams, and Shu Yang, *Water Resource Stress and Food Insecurity in Southern Africa* (Austin: Strauss Center for International Security and Law, August 2011), <http://strausscenter.org/ccaps/climate-vulnerability-publications.html?download=52>; Bonnie Doty et al., *Vulnerability to Climate Change: An Assessment of East and Central Africa* (Austin: Strauss Center for International Security and Law, August 2011), <http://strausscenter.org/ccaps/climate-vulnerability-publications.html?download=53>; Sanjeet Deka, Glakas, Christian, and Olivier, Marc, *Assessing Climate Vulnerability in North Africa* (Austin, Texas: Strauss Center for International Security and Law, August 2011), <http://strausscenter.org/ccaps/climate-vulnerability-publications.html?download=54>.

⁷ *Mapping and Modeling Climate Security Vulnerability: Workshop Report* (Austin, Texas: Strauss Center for International Security and Law, October 2011), <http://strausscenter.org/ccaps/climate-vulnerability-publications.html?download=47.m>

Beyond subnational vulnerability, among the consistent features of our maps are the following attributes: (1) areas of chronic concern (2) relative to the rest of the continent and (3) composite maps of overall climate security concern. These are maps of chronic vulnerability, of perennial places of likely concern, rather than seasonal maps of emergent vulnerability like those produced by the Famine Early Warning Systems Network (FEWS NET).⁸ Unlike some global maps of vulnerability,⁹ our maps are also relative to the rest of Africa, rather than the rest of the world. The least vulnerable parts of Africa may be relatively more or less vulnerable to places outside of Africa, but our area of reference is Africa compared to itself.

Finally, our maps are composite representations of climate security vulnerability. Thus, they are different from maps that seek to chart vulnerability in terms of livelihoods. We have an explicit security focus, emphasizing situations where large number of people could be at risk of mass death from exposure to climate related hazards. Unlike other maps with a similar interest in security, our maps seek to capture that phenomenon in a single integrated composite measure rather than a series of maps each documenting different facets of a problem. For example, Marc Levy at Columbia University and colleagues prepared tables of specific security concerns such as dangerous neighborhoods coupled with specific

⁸ See <http://www.fews.net/Pages/default.aspx>

⁹ Maplecroft, for example, has produced a global climate vulnerability ranking at the subnational level. Maplecroft, "Cities of Dhaka, Manila, Bangkok, Yangon and Jakarta Face Highest Climate Change Risks," November 15, 2012, http://maplecroft.com/about/news/ccvi_2013.html. The Center for Global Development has produced a global vulnerability ranking at the national level. David Wheeler, "Quantifying Vulnerability to Climate Change: Implications for Adaptation Assistance," *Center for Global Development*, 2011, <http://www.cgdev.org/content/publications/detail/1424759/>.

climate risks such as chronic water scarcity.¹⁰ The result is a profusion of tables and maps rather than a single consolidated map that can condense all of the information into a single graphic (which has both strengths and weaknesses).

In our original model, we started with four baskets or processes—physical exposure, population density, household and community resilience, and governance and physical violence—that we thought captured the salient sources of vulnerability, though we recognize that in our aspiration to provide continent-wide maps that some likely indicators of interest (such as road networks) might not be available. Each of these baskets, save for population density, was composed of a number of indicators and we sought sub-national data with fine-grained resolution wherever possible. Our initial index weighted each basket equally and created a composite index by adding the four together. In sensitivity tests, we relaxed that assumption of equal weights.

The methods we have employed to map climate security vulnerability have evolved to reflect the opinions we heard from “ground truthing” our first set of maps with local elites in Africa.¹¹ To date, we have released two major versions of our mapping work, the first 1.0 version is represented by the first working paper we released from the Strauss Center in 2010. Subsequent maps in other published work have largely represented the second iteration 2.0 of our mapping work and

¹⁰ Marc A. Levy et al., “Assessment of Select Climate Change Impacts on U.S. National Security,” 2008, http://www.ciesin.columbia.edu/documents/Climate_Security_CIESIN_July_2008_v1_0.ed.pdf.

¹¹ Berenter, Jared, “*Ground Truthing*” Vulnerability in Africa (Austin, Texas: Strauss Center for International Security and Law, May 2012), <http://strausscenter.org/ccaps/climate-vulnerability-publications.html?download=89>; Berenter, Jared, “*Ground Truthing*” Vulnerability and Adaptation in Africa (Austin, Texas: Strauss Center for International Security and Law, May 2012), <http://strausscenter.org/ccaps/publications/reports.html?download=91>.

extensions and applications. As suggested above, this paper represents the 3.0 version of CSVM, which is a new name that we have christened in this paper.

Part II: An Evolving Methodology

Over the course of the last four years, our efforts to map climate security vulnerability have evolved. This section explains our original model, the changes made in the second iteration 2.0, and then presents the changes made for the current iteration CSVM 3.0.

Vulnerability Model 1.0

To understand what changes we made between the second and third versions of the model, it is helpful to understand where we initially began and what revisions we made between versions 1.0 and 2.0. In the 1.0 iteration of our model, we included several indicators of historic physical exposure to climate related hazards, including floods, fires, drought, cyclone winds, cyclone surge, and low-elevation coastal zones, all of which save for the last one were derived from the UNEP Global Risk Data Platform.¹² With models of future climate change in Africa showing widespread disagreement, the first approximations of the areas likely to face physical exposure to climate related hazards in the future were the areas historically exposed to such hazards. (As an aside, in complementary work, we have

¹² <http://preview.grid.unep.ch/>

collaborated with climate modelers to develop more fine-grained and policy-relevant regional models for Africa).¹³

For population density, we relied on data from Columbia University and the GRUMP model (Global Rural-Urban Mapping Project).¹⁴ In the household basket, we included eight indicators, only two of which included sub-national information (infant mortality and childhood malnutrition). All others (adult literacy, primary school enrollment, life expectancy at birth, drinking water accessibility, healthcare expenditures, and access to nurses and midwives) were at the national level. Finally, our governance basket consisted of two indicators from the World Bank's Worldwide Governance Indicators for 2008, government effectiveness and voice and accountability. We also included two indicators from the Polity IV dataset of political instability through 2008, including the difference between the highest and lowest polity scores in the period 1999-2008 and the number of years since a major change in government (as of 2008). We included a measure of global integration from the KOF Index of Globalization. Finally, we included one sub-national indicator of politically motivated violent events from the Political Instability Task Force for the period 1995-2008.

¹³ See Edward K. Vizy and Kerry H. Cook, "Mid-21st Century Changes in Extreme Events over Northern and Tropical Africa," *Journal of Climate* (March 9, 2012): 120309131130007, doi:10.1175/JCLI-D-11-00693.1; Kerry H. Cook and Edward K. Vizy, "Impact of Climate Change on Mid-twenty-first Century Growing Seasons in Africa," *Climate Dynamics* (March 2, 2012), doi:10.1007/s00382-012-1324-1.

¹⁴ <http://sedac.ciesin.columbia.edu/data/set/grump-v1-population-count>

Changes from the 1.0 to the 2.0 Vulnerability Model

Our 2.0 version of the maps included a number of revisions, including several new data sources and indicators including: (1) a new data source on droughts; (2) a new indicator for areas with chronic low rainfall; (3) an alternate, more fine-grained indicator of population density, (4) a new sub-national indicator of access to improved water sources; (5) a new indicator for sub-national violence; and (6) revised metrics of government effectiveness and voice and accountability which reflect a 3-year weighted average. Here, we explain the changes and rationale for each of them.¹⁵

In terms of drought data, there were two issues. First, the drought indicator in our original model only covered the period 1980-2001, which was a bit dated. Second, it was based on the Standardized Precipitation Index (SPI), which allows you to calculate deviations from normal rainfall but does not pick up on areas of chronic water deficits. Indeed, it is not a very good proxy for drought as this indicator revealed that one of the most “drought-prone” places in the period 1980-2001 in Africa was the northern part of the Democratic Republic of Congo. This area might have had deviations from normal rainfall such that areas that were normally very, very wet became only very wet.

As a consequence of these two observations, we included an updated measure of SPI from the Global Precipitation Climatology Centre (GPCC) for the period 1980-2004. We also added an alternative measure to capture chronic water scarcity based on the coefficient of variation (which is simply the standard deviation

¹⁵ A more detailed discussion of the methodology in the 2.0 model is available as an online appendix for our *International Security* paper.

divided by the mean rainfall).¹⁶ This addition was motivated by our fieldwork where respondents noted that our maps failed to capture areas of chronic water scarcity, already at risk to water shortages and likely to fare worse with climate change.

In addition, we replaced the use of the indicator from GRUMP of population density with a similar measure from LandScan for the year 2008. GRUMP is based on 2000 census data and is based on night-time population whereas LandScan is based on “ambient” populations. LandScan is a modeled dataset based on a variety of inputs such as road networks, elevation, slope, land use/land cover, high resolution imagery. Supporters of LandScan credit it with having more accuracy estimating population concentrations to take into account geographic features such as mountainous areas and rivers.¹⁷

In our quest for more fine-grained data, we also developed a sub-national indicator of access to improved water sources, using the USAID-funded Demographic and Health Surveys (DHS).¹⁸ For some countries, additional subnational data was available through UNICEF’s Multiple Indicator Cluster Surveys (MICS).¹⁹ While this data is collected in the surveys, it takes considerable processing to extract them and have them correspond to specific sub-national administrative units. That meant that the Household and Community Resilience basket had three of eight indicators at the sub-national level.

¹⁶ This helps capture chronic water scarcity quite for the following reason. For areas with low mean rainfall values near zero (like deserts), the value for the coefficient of variation will approach infinity. Small deviations in rainfall will generate large changes in the coefficient of variation.

¹⁷ For differences between GRUMP and LandScan, see <http://sedac.uservoice.com/knowledgebase/articles/41665-what-are-the-differences-between-gpw-grump-and-la>

¹⁸ See <http://www.measuredhs.com/>

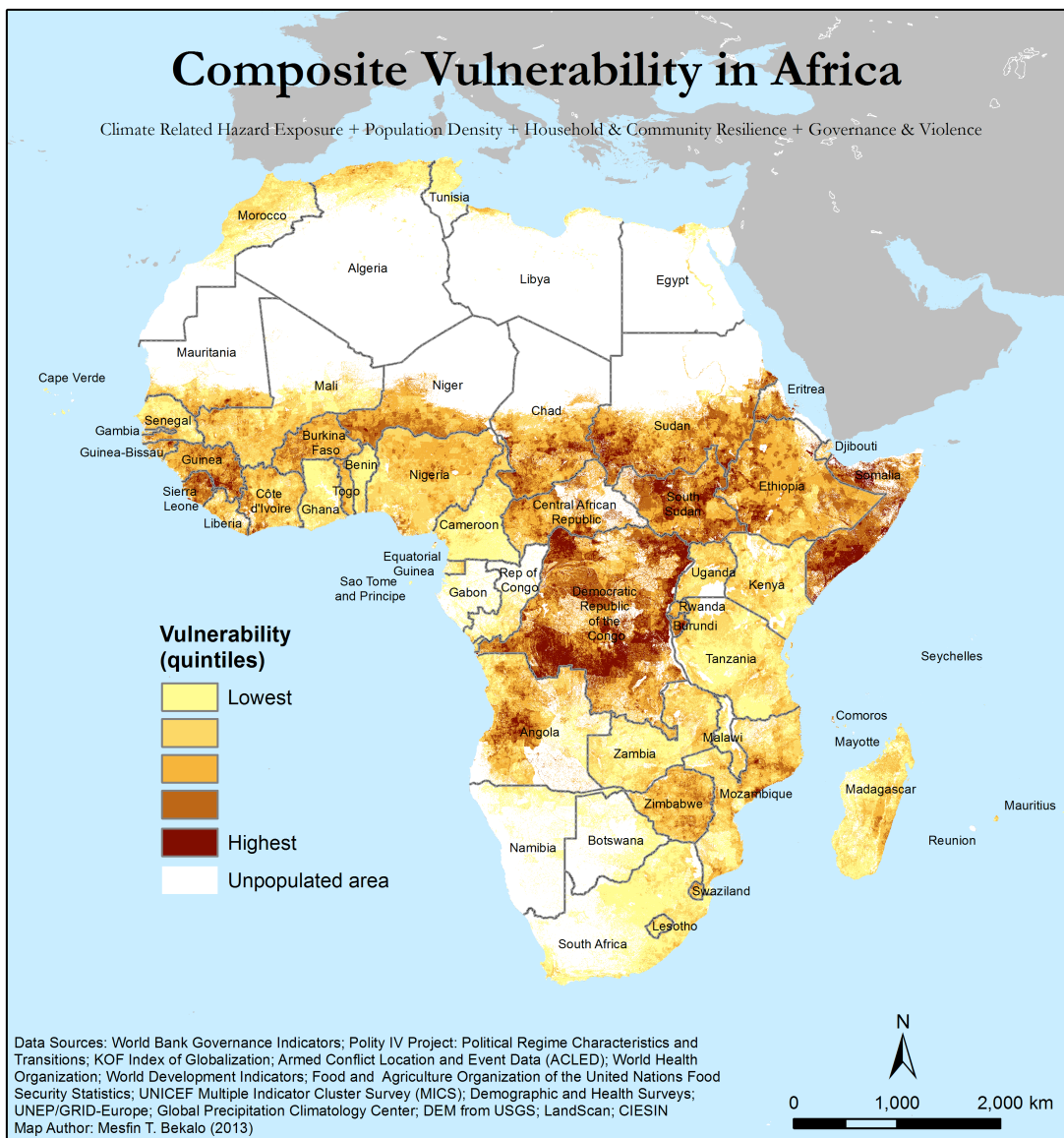
¹⁹ See http://www.unicef.org/statistics/index_24302.html

Finally, in terms of the governance basket, we made several refinements. The data on Worldwide Governance Indicators initially reflected a single year 2008, but this is an indicator with some flux and variability, meaning that a value from a single year could drive the results for our measures of government effectiveness and voice and accountability. We therefore chose to create a three-year weighted average, weighting the most recent year 2009 the most (50%), the previous year 2008 second (30%), and two years prior 2007 the least (20%). We also substituted for the Political Instability Task Force indicator of atrocities against civilians a broader measure of conflict from the Armed Conflict and Event Location Dataset (ACLED) for the period 1997–2009. These were assigned to the lowest administrative unit possible to create a frequency count of violent events. The idea here was that governments might not be willing or able to extend aid and assistance to places with a history of violence and conflict in the event of a climate related emergency.

In the base composite vulnerability model, all four baskets were weighted equally and added together. Each indicator was “normalized” into a common scale. We classified them into categories on a scale from 1 to 5, with 1 being the most favorable and 5 being the worst outcome. In the climate related hazard basket, areas with extremely low rainfall are represented by a separate category of 0. In the population density basket, unpopulated areas were represented by a separate category of zero. When we added all four baskets together for the composite map of overall vulnerability, these unpopulated areas were excluded. In some iterations of the 2.0 model, we relaxed the assumption of equal weights to the baskets to see how the maps changed with different weights attached to the baskets. Figure 1 shows the

map results for the 2.0 version of our model which shows high vulnerability across Somalia, Sudan and South Sudan, pockets in the Democratic Republic of the Congo (DRC), and in Guinea and Sierra Leone (see Figure 1).

FIGURE 1: COMPOSITE VULNERABILITY MAP 2.0



Changes from the 2.0 to the 3.0 Vulnerability Model

We made a number of changes to the indicators and approach in version 3.0 of the CSVM, related to the units of analysis, the normalization of data, and the functional form of the model.

Units of Analysis

We sought subnational data wherever possible for use in the model. For a number of indicators, particularly in the Household and Community Resilience basket, we used USAID Demographic and Household Surveys to calculate subnational data. In our previous work, we relied on shapes of subnational units using the data from Global Administrative Areas dataset (GADM).²⁰ Other available options include data from the Global Administrative Unit Layers (GAUL)²¹ and Map Library. As we endeavored to mine the DHS data for this third iteration of our maps for more subnational indicators of interest, we discovered that DHS shapes and GADM do not always neatly coincide. Moreover, we discovered that GADM does not always have files available for the current political divisions of some countries.

For example, in the case of Ghana, GADM has 137 local governments units, but Ghana has reorganized and now has 170 local government units. In the case of Ghana, we now rely on GAUL for the subnational administrative boundaries, of which there are 10 level one administrative units. Our preference was to use the most recent data, wherever possible, or should two data sources be roughly similar in vintage, we rely on the data source that has borders that fit well with neighboring

²⁰ <http://www.gadm.org/>

²¹ <http://www.fao.org/geonetwork/srv/en/metadata.show?id=12691>

countries, since location of borders may vary slightly by data source. As a consequence, based on the latest shape files that are available from various sources, we created our own master shapefile for all level one administrative boundaries across Africa, typically corresponding to regional boundaries of states or provinces.

Normalization

The five-category scale 1 to 5 that was used in previous iterations had some disadvantages. We lost a lot of information collapsing the numbers into five whole numbers. Such a normalization exercise made it easy to visualize the data, but it proved less useful for trying to understand if a particular point lies closer to one whole number or another. Moreover, if we wanted to alter an underlying indicator and see what effect an improvement in, say infant mortality, had on overall vulnerability, having five categories was a blunt instrument. Moreover, our 1 to 5 ranking scheme was meant to capture the range of values from the least vulnerable 20% (a score of 1) to the most vulnerable 20% (a score of 5). In reality, in addition to the loss of information from the 1 to 5 scale, there was quite a lot of clustering so that these quintiles were not evenly distributed, making it harder to interpret what the scores meant.

As a consequence, in this version of the data, all indicators were normalized on a scale from 0 to 1 to three decimal places, using percent rank (a version of dispersion between the minimum and maximum)²² or percentiles.²³ This gives us a

²² We converted the percent rank to show where a given value is in percentage terms between the minimum and maximum score as represented by the equation $\text{minmax} = 1 - (\text{value} - \text{min}) / (\text{max} - \text{min})$

more variegated scale to work with. Instead of 5 whole numbers, we now have a scale to two or in some cases three decimal places with low scores approaching 0 representing maximal vulnerability and high scores approaching 1 representing no vulnerability (high overall resilience). In the legends of the composite maps, we now present the range of values on a zero to 1 score rather than quantiles.

Functional Form

In addition, in this paper, we again start with an additive index with all four baskets equally weighted.

Model 1: CSVM additive

$$= (\text{Climate Related} + \text{Population Density} + \text{Household Resilience} + \text{Governance})$$

As a reviewer to one of our previous studies pointed out, a location with a low or zero score on climate exposure could still record a high value on climate security vulnerability if the other three baskets have high values. If the base nature of the model is supposed to be related to climate change, then having no physical exposure should have some impact on the overall vulnerability, notwithstanding the high values of the other three baskets. To this end, in this iteration of the model, we also experiment with a multiplicative version of the model where the composite score rises to 1 if there is no climate related exposure.

Model 2: CSVM multiplicative

$$= \text{Climate Related} \times (\text{Population Density} + \text{Household Resilience} + \text{Governance})$$

²³ Percentiles reflect the percentage of scores below a certain number. The equation representing percentiles is total number of values below X/ total number of values.

In this paper, we employ both additive and multiplicative versions of the model for comparison.

In addition, we consider an alternative way to account for population. Rather than have a separate basket, we consider an alternative where we weight the final composite map by population. The rationale here is to deflate each basket by population so that the indicators drop towards no exposure the less densely populated the area is.

Model 3: CSVM additive popweight

$$= (\text{Pop} * \text{Climate Related} + \text{Pop} * \text{Household} + \text{Pop} * \text{Governance})$$

Finally, we consider a combined version where both population and climate hazard exposure are multiplied by the other terms such that if either no one lives in a location or there is no climate hazard exposure, the composite index would register no vulnerability.

Model 4: CSVM multiplicative popweight

$$= (\text{Pop} * \text{Climate Related}) * (\text{Pop} * \text{Household} + \text{Pop} * \text{Governance})$$

Climate Related Hazard Exposure

As for changes in individual indicators, in terms of the physical exposure basket, we were able to update a number of data sources and develop some new indicators. As Table 1 demonstrates, we include indicators for rainfall anomalies, chronic water scarcity, cyclones, wildfires, floods, and low-lying coastal zones. These correspond to the same concepts we applied in our model 2.0, but in a number of cases, we have replaced the indicator with either an improved data source, an

updated set of newer data, or at the very least, the data has been normalized on a 0 to 1 scale rather than a 1 to 5 scale as before.

TABLE 1: CLIMATE RELATED HAZARDS DATA SOURCES

Table 1. Indicators Used to Assess Physical Exposure to Climate Related Hazards				
Hazard Type (weight)	Indicator	Scale	Years of Data Used	Source
Cyclone Winds	Tropical cyclones average sum of windspeed (km per year)	2 km x 2 km resolution	1970-2009	UNEP/GRID-Europe
Floods	Flood Frequency (per 100 years)	1 km x 1 km resolution	1999-2007	UNEP/GRID-Europe
Wildfires	Estimated frequency of events	1 km x 1 km resolution	1995-2011	UNEP/GRID-Europe
Aridity	Monthly coefficient of variation	0.5 degree	1980-2009	Global Precipitation Climatology Centre
Rainfall scarcity	Number of months between 1980-2009 in which the 6-month accumulated rainfall was 1.5 standard deviations or more below the average for that calendar month over the previous 20 years.	0.5 degree	1980-2009	Global Precipitation Climatology Centre
Inundation (Coastal elevation)	Low-lying coastal areas within 0 to 10km above sea level	10m x 10m resolution		USGS DEM

In terms of rainfall-related indicators, we were not satisfied that the representation by the Standardized Precipitation Index in the form we previously used was that meaningful. The previous version relied on a count of events and intensity over the entire period 1980-2004.²⁴ Previous studies had suggested that this indicator did a somewhat decent job mirroring patterns of drought, as represented in the EM-DAT disaster database. As our composite model is meant to

²⁴ The drought data are represented by a raster with values based on the six-month standardized precipitation index (SPI) according to the severity of drought in a given calendar year. If the SPI does not drop below -1 for at least three consecutive months, the value is set to zero. If the six-month SPI does drop below -1 for at least three consecutive months, the value is set to 1; if it is below -1.5 for at least two consecutive months, the value is set to 1.5. If both criteria are met, the value is set to 2.5.

pick up on other risks that contribute to the occurrence of disasters, we want a measure of negative changes in rainfall that is purely physical that together with other indicators should contribute to disaster vulnerability. Rather than create a frequency count over the entire period of study, we created a rolling twenty-year average based on the accumulated rainfall for the previous 6 months. The idea here is that people, particularly farmers, will have some appreciation of what the rainfall should look like over a given period (in this case, the previous six months). The memories of adults may stretch back about twenty years. Thus, if the accumulated rainfall deviates strongly from the previous patterns over the last twenty years, this could have a major impact on water users' (including farmers) ability to plan, plant, and execute their operations, with knock-on disruptive consequences. Using data from the Global Precipitation Climatology Centre (GPCC), we therefore calculated whether or not a given six-month period deviated strongly from the twenty-year average for the same six months. We were able to generate such a rolling six-month standardized precipitation measure for the period 1980-2009.²⁵

As in version 2.0, to get at places with chronic water scarcity, we also calculated the average monthly coefficient of variation. Again, we used GPCC data, and here, we were able to update the data for the period 1980-2009. For both of these indicators, we were able to generate values across the entire continent. In the previous iteration, we received data that suggested rainfall was too low to calculate the SPI or CV across wide swathes of area in the Sahara. Those areas were excluded from the physical exposure basket, lest they skew the rankings. Including those

²⁵ This is defined as the number of months between 1980-2009 in which the 6-month accumulated rainfall was 1.5 standard deviations or more below the average for that calendar month over the previous 20 years.

areas but recording a zero for them would have potentially indicated no physical exposure, which would not be right. They did not have enough rainfall to register droughts but were areas that faced perennial water scarcity. While they might not face changes in the climate, the climate conditions were already harsh.

For the cyclone indicator, we elected to use a new indicator from the UNEP/GRID-Europe platform called “sum of winds.” It is meant to capture both frequency and speed of cyclone events, thus providing some measure of event intensity. It is measured in kilometers/year. This gave us values for the period 1970-2009. The rationale here was that in our prior version, we had created our own weighting scheme for different categories of cyclones based on the frequency of cyclone severity, giving extra weight to more extreme cyclone events. This weighting scheme and reclassification into five categories was somewhat arbitrary,²⁶ and we preferred to rely on a measure created by subject area experts explicitly for the purpose of bringing together frequency and severity of cyclone events. Use of this indicator allowed us to bring in two years of additional data for the period 1970-2009.

Since our original use of the UNEP/GRID-Europe data on physical hazards, they also updated other data sources, including wildfires. We now map wildfires for the period 1995-2011, which provides several additional years of data.

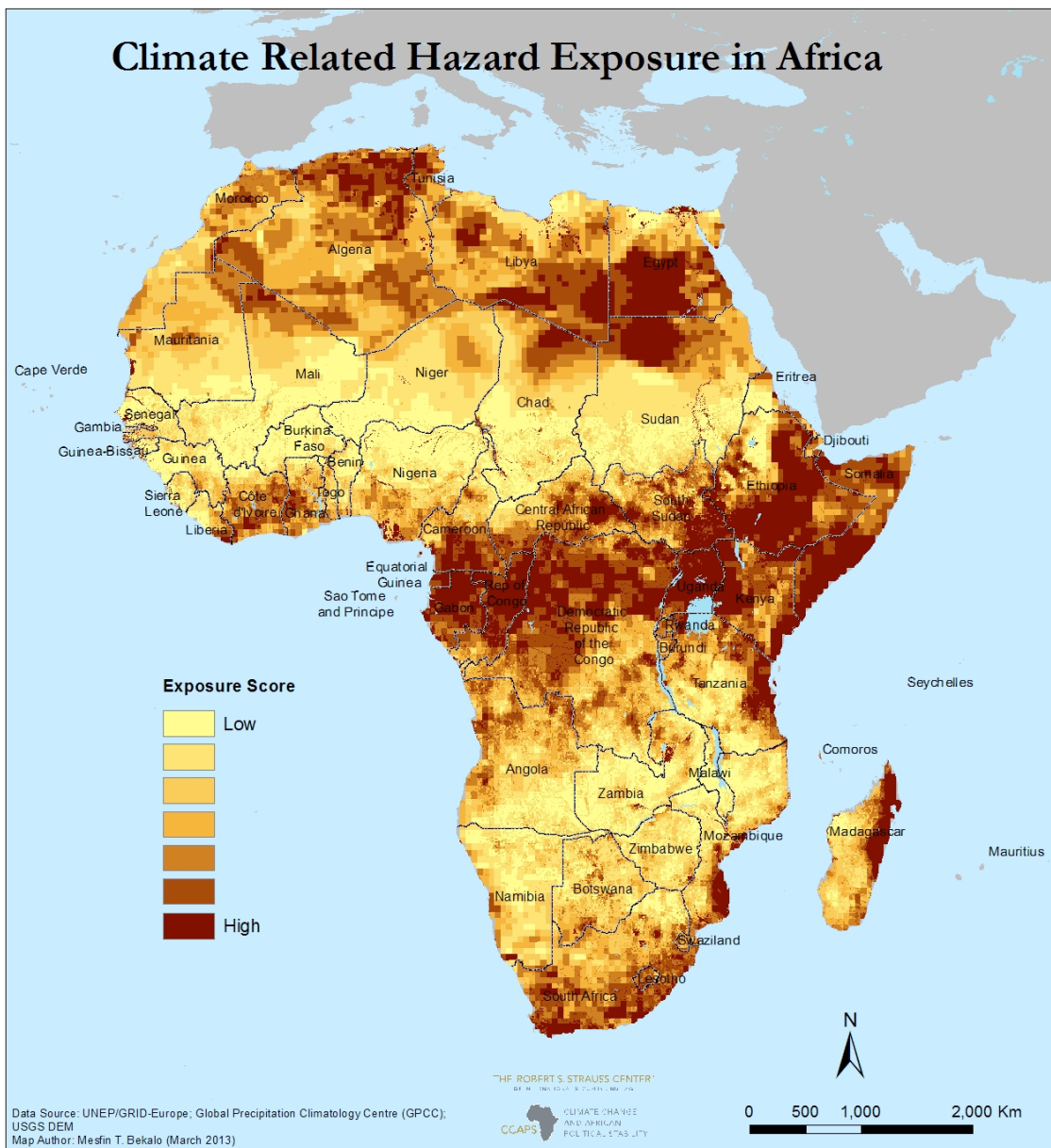
In terms of the other indicators, the raw flood data and the low-elevation coastal zones indicator remained unchanged from the previous iteration of the

²⁶ These scores are represented as a final cyclone frequency raster using the following equation: cyclone wind frequency = category 1 frequency + (category 2 frequency * 2) + (category 3 frequency * 3) + (category 4 frequency * 4) + (category 5 frequency * 5). This formula assigns greater weight to stronger, more dangerous cyclones.

model. However, for all indicators, we normalized the data on 0 to 1 scale with three decimal places. In this iteration of the model, given that both rainfall anomalies and chronic water scarcity indicators were meant to capture similar phenomena related to the effects of changes in rainfall, we divided the weight between them. Where floods, cyclones, wildfires, and low-lying coastal zones each represented 20% of the overall climate related hazard or physical exposure basket, that 20% was split equally between water anomalies (6 mo. standardized precipitation measure) and chronic water scarcity (CV).

Combining these indicators into a single basket map of climate related hazard exposure yields a map showing a band of high physical exposure extending from Somalia through Ethiopia and South Sudan, extending across parts of the Democratic Republic of Congo and Congo and including parts of Gabon and Cameroon. In North Africa, parts of Egypt and northern Sudan, along with parts of Tunisia and Algeria face high exposure. In Southern Africa, the eastern edge of Madagascar, coastal Mozambique, and pockets in South Africa also face high exposure (see Figure 2).

FIGURE 2: CLIMATE RELATED HAZARD EXPOSURE



Population Density

In the 2.0 iteration of our maps, we used the Landscan values for 2008 and converted them into quintiles. In this version 3.0, we use 2011 data for Landscan and normalize the data into percentiles on a zero to 1 scale (see Table 2).

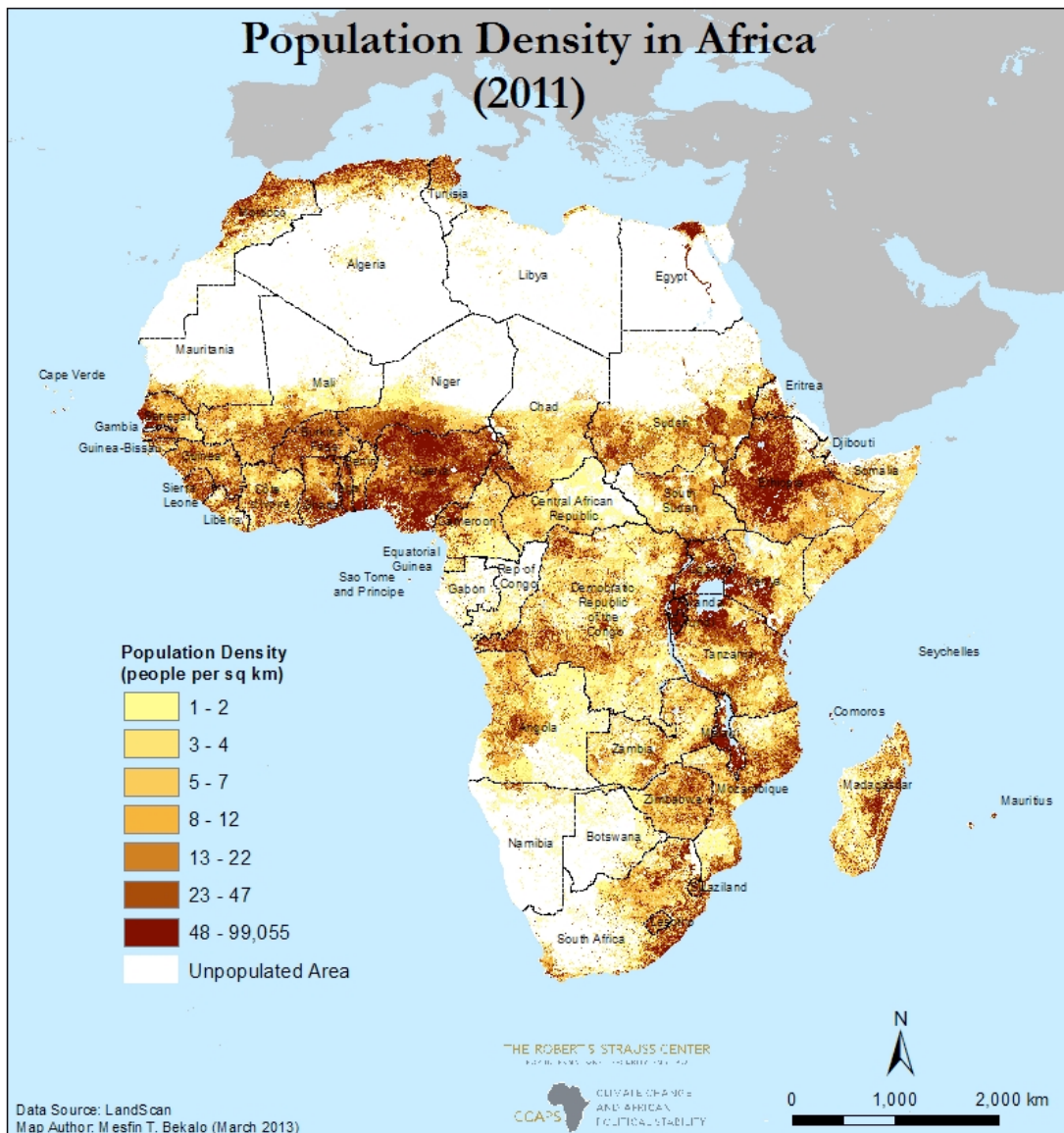
TABLE 2: POPULATION DENSITY DATA SOURCES

Table 2. Indicators used to Assess Population				
Variable	Indicator	Scale	Years of Data Used	Source
Population Density	Ambient population (average over 24 hours)	Subnational at 1 km x 1 km resolution	2011	LandScan Oak Ridge National Laboratory

As Figure 3 shows, population concentrations are found in western Ethiopia, throughout Nigeria and neighboring coastal West Africa, in and around the Great Lakes region, Egypt, along Lake Malawi, and across parts of the Mediterranean coastline of Morocco and Tunisia. It should be noted that in the map below, the range of the most densely populated areas (dark brown) is enormous, from 48 people per square kilometer to 99,055 per square kilometer.

Most of the values continent wide are lower than 50 people per square kilometer, and the highest population concentrations (50,000 people per square kilometer or more) are in a handful of places, in and around major cities in Egypt (Cairo, Alexandria) and Morocco (Fez, Meknes, Rabat, Casablanca), as well Algiers; several cities in Nigeria (including Lagos, Ibadan, Akure, Asaba), several other West Africa cities (Abidjan, Lome, Cotonou), several cities in Central and East Africa (Kinshasa, Brazzaville, Addis Ababa, Nairobi, Kampala, Dar es Salaam), as well as several cities in Southern Africa (Maputo, Durban).

FIGURE 3: POPULATION DENSITY



Household and Community Resilience

In version 2.0, this basket contained four categories of paired indicators for a total of eight: two for education, two for health, two for daily necessities, and two for access to healthcare. Of these, only three contained subnational information, infant mortality, underweight children, and access to improved drinking water sources. In

this iteration of the maps, we obtained updated infant mortality data, normalized to the year 2008, obtained from ISciences.²⁷ In addition, we derived new subnational data for literacy and school enrollment from the USAID DHS surveys and the UNICEF MICS surveys. We also updated data on access to improved water sources and underweight children to take advantage of new DHS and MICS surveys. Finally, we have some subnational information for delivery in health facility from those same surveys, which we thought of as a better proxy for access to health services than our existing national indicator of the number of midwives and nurses.²⁸ What this means is that we now have subnational indicators for six of eight indicators in this basket (see Table 3).

²⁷ Global Climate Change Research Program (2011). Global Subnational Infant Mortality Rates ca. 2008. Environmental Indications and Warnings Project. Central Intelligence Agency. U.S. Government.

²⁸ DHS administrative regional boundaries did not always correspond neatly to our level one administrative regions, with borders off slightly. We were able to match these in most cases by using the centerpoint of our regions and applying the value from the DHS regions to our shapes. In the case of Burkina Faso and Rwanda, the differences between DHS regions and our shapes were more severe, with multiple DHS regions corresponding to one of our regions. In such cases, we made a decision to apply a value to our shape that was roughly representative of the DHS values for those regions (for example, if there were three values, we took the intermediate one).

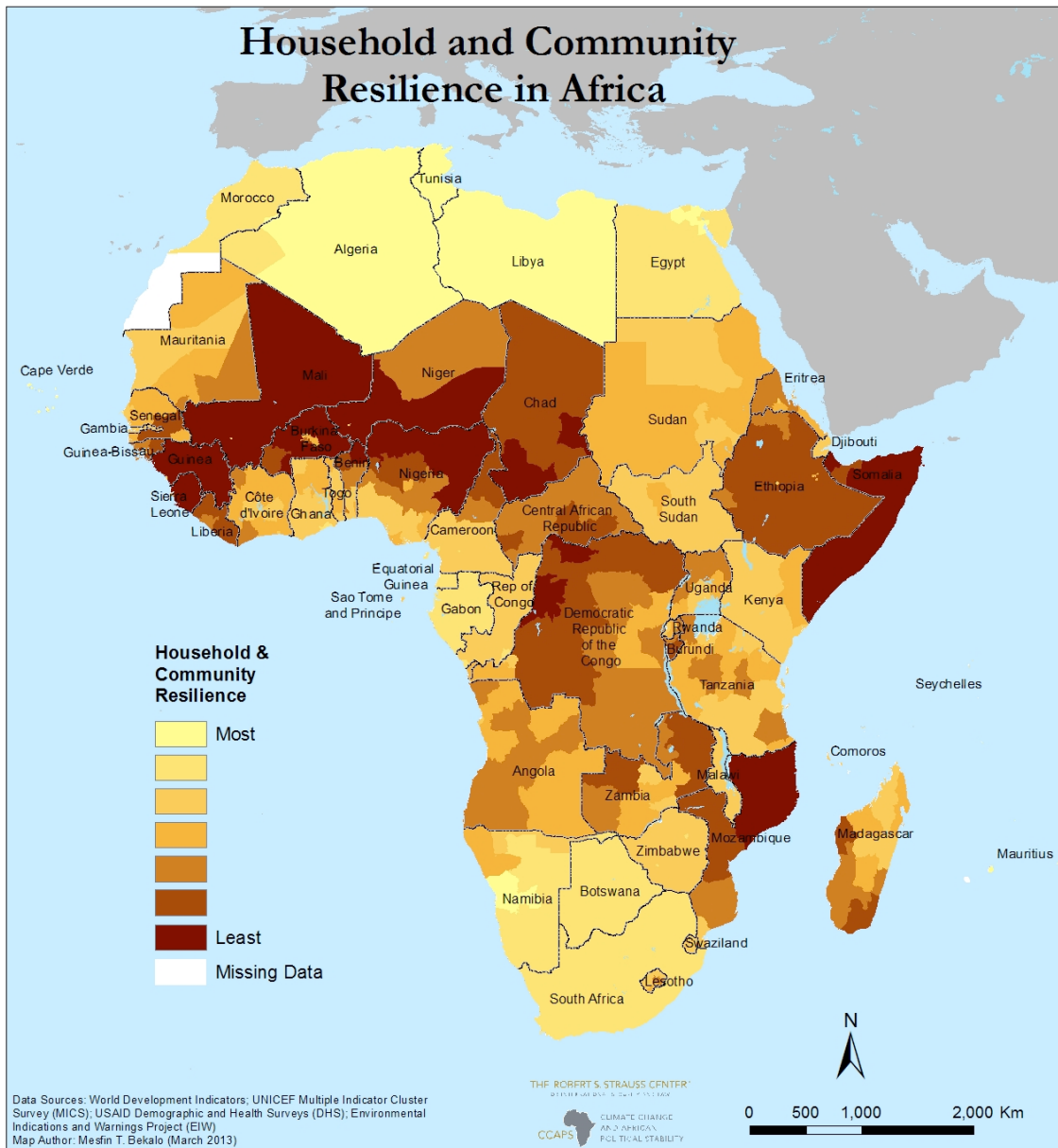
TABLE 3: HOUSEHOLD RESILIENCE DATA SOURCES

Table 3. Indicators Used to Assess Household and Community Resilience				
Category	Indicator (weight)	Scale	Years of Data Used	Source
Education (25%)	Literacy rate, adult total (% of people ages 15 and above) (12.5%)	National, CCAPS First Administrative District	DHS 2003-2011, Stats SA 2011, World Development Indicators (WDI) 2006-2010	Subnational data from DHS, MICS; Stats SA national level data WDI
	School enrollment, primary (% gross) (12.5%)	National, CCAPS First Administrative District	DHS 2003-2011, Stats SA 2011, MICS 2006-2010, UNICEF 2003-2008	Subnational data from DHS, MICS; Stats SA, national level data UNICEF
Health (25%)	Infant mortality rate adjusted to national 2000 UNICEF rate (12.5%)	CCAPS First Administrative District	2008	Environmental Indications and Warnings Project
	Life expectancy at birth (years) both sexes (12.5%)	National	2008, 2010, 2011	WDI
Daily Necessities (25%)	Percentage of children underweight (more than two standard deviations below the mean weight-for-age score of the NCHS/CDC/WHO international reference population (12.5%)	National, CCAPS First Administrative District	DHS 1999-2010, WDI 2000, 2004-2008, 2011	Subnational data from DHS; national level data WDI
	Population with sustainable access to improved drinking water sources total (%) (12.5%)	National, CCAPS First Administrative District	DHS 2003, 2005-2011, MICS 2006-2007, 2010, Stats SA 2011, WDI 2001, 2006, 2008-2010	Subnational data from DHS, MICS, Stats SA; national level data WDI
Access to Healthcare (25%)	Health expenditure per capita (current US\$) (12.5%)	National	WDI 2001, 2010	WDI
	Delivery in a health facility (% of births) (12.5%)	National, CCAPS First Administrative District	DHS 1999-2008, 2010, UNICEF 2003-2008	Subnational data from DHS, UNICEF; national indicators from UNICEF

All of these data sources were converted into percent ranks and normalized on a zero to one score. All four categories received equal weight in the index of 25%. Each indicator in the category would thus receive 12.5% of the weight of the whole basket. In the event a particular indicator was missing data, the other indicator would take on the full 25% category weight.

Combining all these indicators in a single map yields Figure 4 which shows that the least resilient areas of the continent are located in Somalia, Nigeria, and across the Sahel while the most resilient areas (the areas where communities have the highest levels of education, better health conditions, access to necessities and health services) are located on the island of Mauritius and primarily in North Africa, including Tunisia, Algeria, Egypt, and Libya.

FIGURE 4: HOUSEHOLD AND COMMUNITY RESILIENCE



Governance and Political Violence

The 2.0 version of our maps contained five categories of indicators and six indicators. We included indicators of government responsiveness, government response capacity, openness to external assistance, two indicators for political stability, and presence of violence. Of these, only one contained subnational

information. In CSVM 3.0, these indicators have been updated to include more recent data (see Table 4). In North Africa, this is particularly important since the region experienced historic transformations in political stability after the introduction of our version 2.0.

In version 3.0, we now have indicators for government effectiveness and voice and accountability through 2011 (previously these indicators covered the period 2007-2009). Again, we represent these indicators through a diminishing weighted-average for the period 2011 dating back to 2008.²⁹

The indicator for openness to external assistance from the 2009 KOF Index of Globalization remains unchanged, as we believe this to be a slow-changing indicator.

In terms of political stability, we took advantage of the release of new Polity IV data through 2011. Our indicator of polity variance now covers the period 2002-2011 (it previously covered the period 1999-2008).

Finally, as before, our sole subnational indicator in this basket is the Armed Conflict and Location Events Dataset (ACLED). The measure here encompasses all categories of ACLED events for the period 1996-2012 (in the previous iteration, we had events for the period 1997-2009). In this iteration, we place more weight on recent events compared to more distant ones.³⁰ In version 2.0, we attached ACLED events to the smallest administrative unit where available, since the original data was point data. However, for the purposes of creating a consistent percentile rank

²⁹ The value is a diminishing weighted average with 2011 assigned the most weight (.4), followed by 2010 (.3), 2009 (.2), 2008 (.1). Expressed in percent rank.

³⁰ The weighting function is as follows: $\text{gen wt_evnts} = ((1/16) * v5) + ((2/16) * v6) + ((3/16) * v7) + ((4/16) * v8) + ((5/16) * v9) + ((6/16) * v10) + ((7/16) * v11) + ((8/16) * v12) + ((9/16) * v13) + ((10/16) * v14) + ((11/16) * v15) + ((12/16) * v16) + ((13/16) * v17) + ((14/16) * v18) + ((15/16) * v19) + ((16/16) * v20)$. v5 is 1997 and v20 is 2012. This means that events in 2012 gets a full weight of 1 but that diminishes by 1/16 each year until 1997 which gets a weight of only 1/16.

across all subnational administrative units, we needed to have consistent units of analysis across different subnational indicators. We therefore elected to aggregate ACLED events to the level one administrative unit, again corresponding to regional boundaries in most cases.³¹

TABLE 4: GOVERNANCE DATA SOURCES

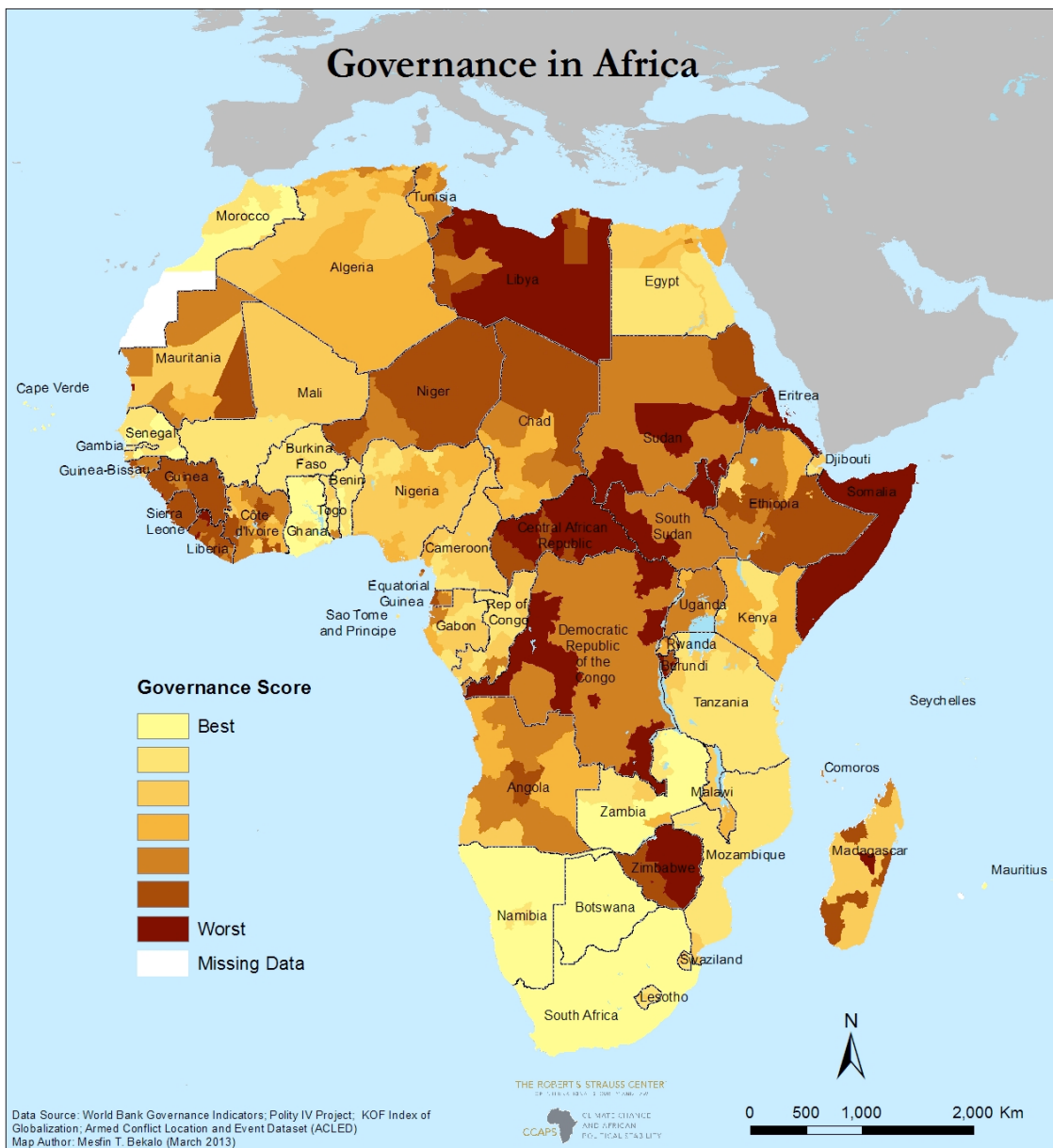
Table 4. Indicators used to Assess Governance and Violence				
Category	Indicator (weight)	Scale	Years of Data Used	Source
Government Responsiveness	Voice and Accountability (20%)	National	2008, 2009, 2010, 2011	WDI
Government Response Capacity	Government Effectiveness (20%)	National	2008, 2009, 2010, 2011	WDI
Openness to External Assistance	Globalization Index (20%)	National	2009	KOF Index of Globalization
Political Stability	Polity Variance (10%)	National	2002-2011	Polity IV Project
	Number of Stable Years (as of 2011) (10%)	National	1855-2011	Polity IV Project
Presence of Violence	Subnational conflict events (20%)	CCAPS First Administrative Division	1997-2012	Armed Conflict Location and Events Database (ACLED)

Combining these indicators into a single map yields Figure 5, which shows that the areas with the worst governance include most of Somalia, pockets in both South Sudan, Sudan, parts of the Democratic Republic of the Congo, as well as much of Libya (picking up on civil war and political instability after the Arab Spring), as well as the Central African Republic (which in March 2013 experienced a coup). By contrast, areas with the best governance scores include several island countries

³¹ The other reason for using all level one administrative units was that the smaller the administrative unit that you use, the fewer events, all else equal, that were likely to take place in a given unit. If a reasonably large level one administrative unit has many conflict events distributed across it, using a smaller administrative unit would then divvy up that larger pool of conflict events among the smaller units, making it appear that a country was less conflict-ridden relative to other geographic units.

(Mauritius, Cape Verde, the Seychelles) as well as much of Botswana, pockets in Morocco (in the Sud region), Namibia, Ghana, and South Africa.

FIGURE 4: GOVERNANCE



Part III: Findings

We combine all four baskets together using four different methods: (1) our original additive function (2) a multiplicative model, a (3) population-weighted

version of the additive model, and (4) a population-weighted version of the multiplicative model. In this section, we present maps of the four variants of the composite map and compare the findings with the 2.0 version of our maps. Below, we summarize the four basic equations for the models.

Model 1: $\text{CSVM}_{\text{additive}} = C + P + H + G$

Model 2: $\text{CSVM}_{\text{multiplicative}} = C * (P + H + G)$

Model 3: $\text{CSVM}_{\text{additive, pop-weighted}} = P * C + P * H + P * G$

Model 4: $\text{CSVM}_{\text{multiplicative, pop-weighted}} = (P * C) * (P * H + P * G)$

C = climate related hazard exposure

P = population density

H = household and community resilience

G = governance

In order to retain the zero to one scale (with zero meaning maximal vulnerability and 1 meaning no vulnerability), we had to re-normalize the data, dividing by the total possible score.

Model 1: $\text{CSVM}_{\text{additive}} = (C + P + H + G)/4$

For both the multiplicative and the population-weighted versions of the index, we wanted to have the areas with no exposure or no population register no vulnerability. Since our value for no exposure or population was 1, we calculated the inverse score for all our indicators, which would give us zeroes for areas with no exposure (model 2), zeroes for no population (model 3), and zeroes for areas with either no exposure or no population (model 4). We then subtracted the composite score from one and divided by the total possible score to re-normalize on a zero to 1

scale, with 1 being no vulnerability (high overall resilience). The equations used for models 2 through 4 were therefore:

Model 2: $\text{CSVM}_{\text{multiplicative}} = 1 - ((1-C) * ((1-P) + (1-H) + (1-G))) / 3$

Model 3: $\text{CSVM}_{\text{additive pop-weighted}} = 1 - ((1-P) * (1-C) + (1-P) * (1-H) + (1-P) * (1-G))$

Model 4: $\text{CSVM}_{\text{multiplicative pop-weighted}} = 1 - ((1-P) * (1-C) * ((1-P) * (1-H) + (1-P) * (1-G)) / 2)$

Figures 5-8 show the maps for all four model permutations. Models 1 and 3 (Figures 6 and 8) are similar as are models 2 and 4 (Figures 7 and 9). Models 1 and 3 show extensive vulnerability across the Horn of Africa (particularly in Somalia and Ethiopia), in pockets around the Great Lakes in Uganda and Burundi, with higher areas of vulnerability through Nigeria and southern Niger, as well as West Africa in Guinea and Sierra Leone. Model 3 (Figure 8) accentuates the vulnerabilities of densely populated locations with unpopulated areas in the Sahara and Kalahari deserts dropping to the lowest vulnerability in light yellow. Areas with extremely low climate exposure nearly drop out in models 2 and 4, reducing the number of places with high vulnerability to a handful of places: Somalia, coastal areas in Madagascar, Mozambique, Nigeria, and Mauritania; Egypt; pockets in the Ethiopian highlands, central Uganda, and Algeria (Figures 7 and 9).

FIGURE 6: MODEL 1

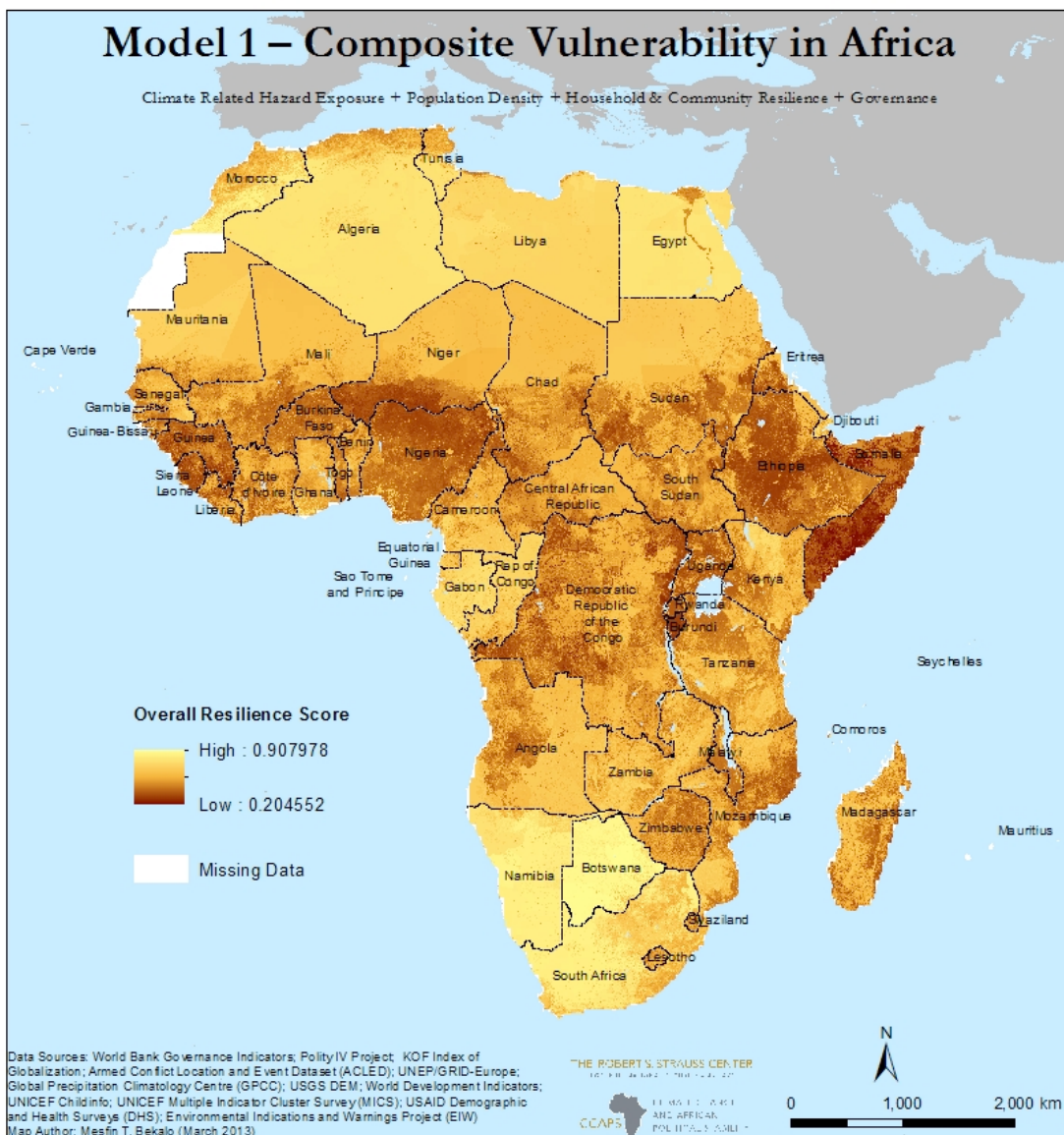


FIGURE 7: MODEL 2

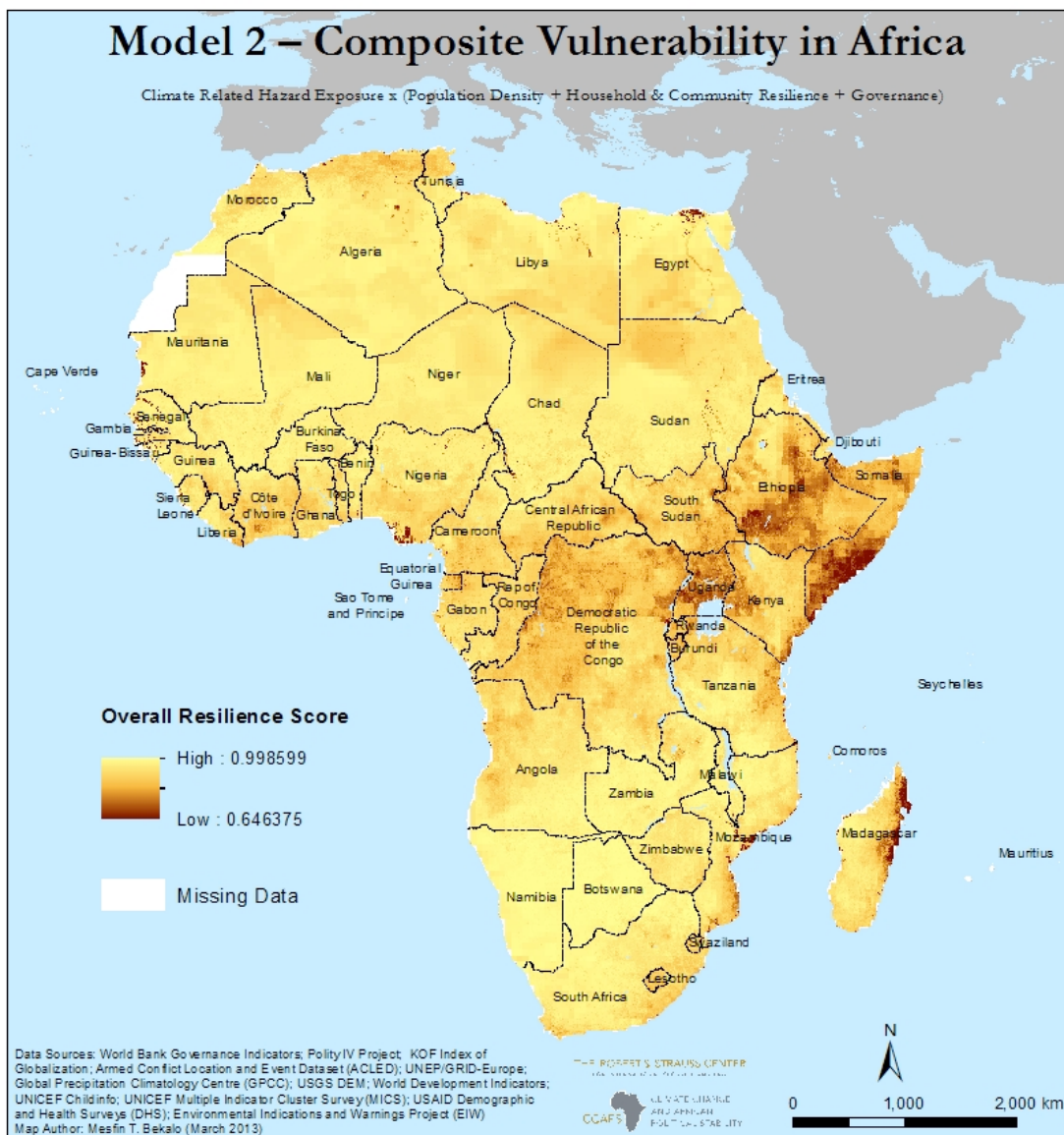


FIGURE 8: MODEL 3

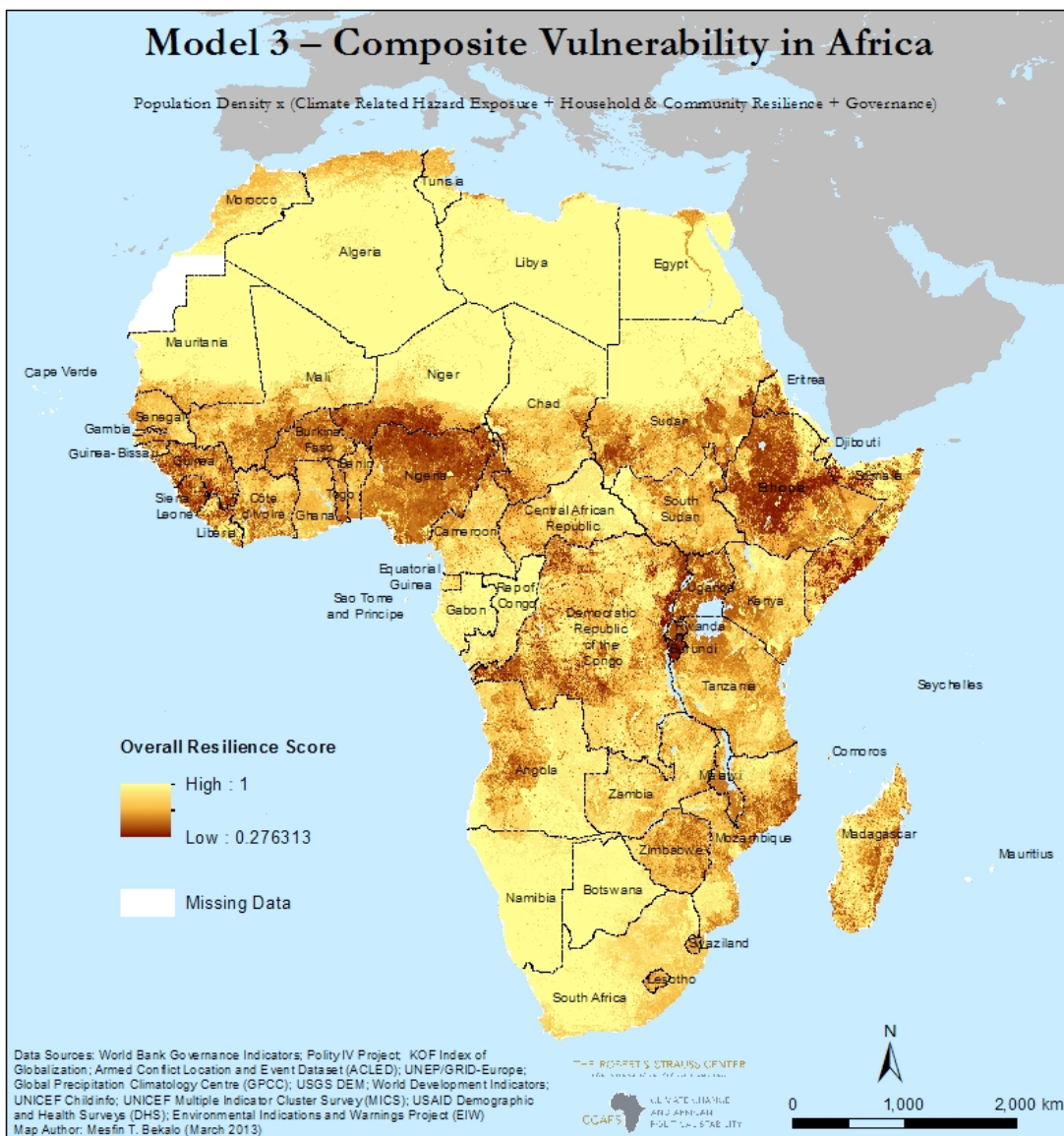
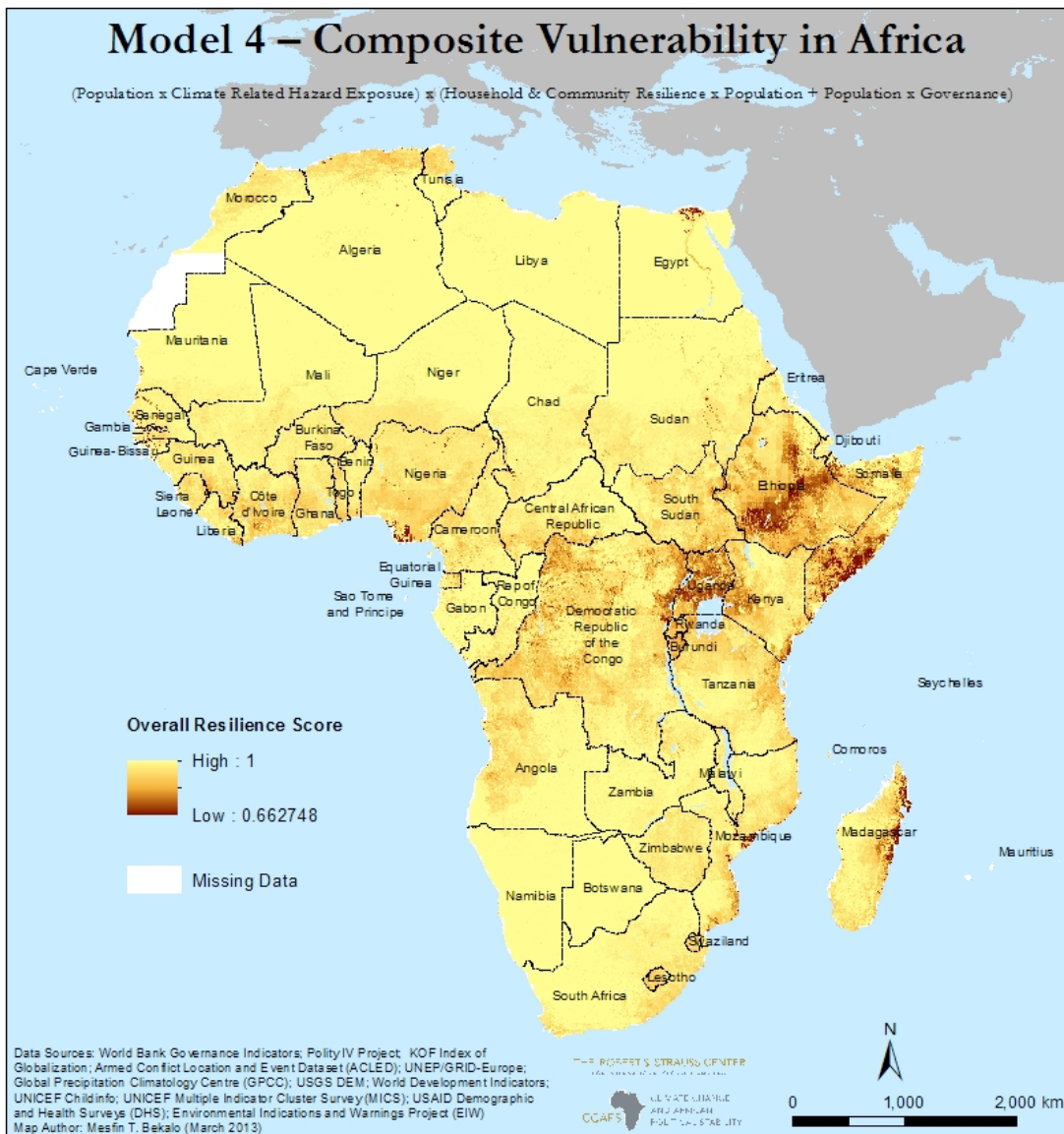


FIGURE 9: MODEL 4



Comparison of CSVM 3.0 with Version 2.0

The patterns we observe in the basic 3.0 additive Model 1(Figure 6) are somewhat different from the 2.0 model results (see Figure 1). Somalia, western Ethiopia, and pockets in West Africa (in and around Guinea and Niger) retain their high vulnerability. Patterns in the DRC are similar, though somewhat diminished.

With an overall score and stretched representation of our results on 0 to 1 scale, the portrait of vulnerability in CSVM 3.0 is more evenly distributed across the continent compared to the 2.0 model which collapsed values into five categories.

Part IV: Implications and Extensions for Future Research

In light of these findings, one of the more challenging questions is the extent to which we can trust the maps as indicative of any real phenomena in the world, especially since the patterns are somewhat different than what we developed in the 2.0 iteration of our maps and because there are sharp differences between them. In addition to sensitivity tests of how much the model findings change with different functional forms, we want to know something more about the model's external validity: are the locations we find most vulnerable the same ones that come up in other studies?

Here, we need a relevant comparison set of data that were compiled by others but for similar purposes. To the extent that the patterns we observe in our maps mirror those of others, we are likely to have more confidence that our maps represent an underlying reality. At the same time, given that our four models show some different patterns for the locations of vulnerability, the comparison with other data can provide us with some guidance about which of our models is the best.

Our goal is to identify places where large number of people could be exposed to mass death from climate related hazards. Here, the EM-DAT International Disaster Database compiled by the Université Catholique de Louvain in Belgium may be a suitable candidate for assessing the external validity of our model. The EM-DAT

database records situations that already rise to a certain level of damage to be included in the database.³² Since EM-DAT events represent negative outcomes where physical exposure intersects with where people live, what resources they have to protect themselves, and how their governments respond, it is a decent proxy for what we are trying to explain. Their database includes a variety of climate related “disasters.”³³ The geographic coordinates in EM-DAT are not very precise – usually a field will list a town or province name, several provinces or regions, or sometimes the country as a whole. While EM-DAT has had a decade-long discussion about more accurate geocoded information,³⁴ they have yet to resolve methodological issues to release a geo-coded version of their own.

We geo-coded these events for the period 1997-2012 by linking them to our CCAPS level-one administrative regions with individual events sometimes linked to more than one region or even the country as a whole.³⁵ In Figure 10, we plot the patterns of frequency counts of climate related disaster events, and we can compare them to the patterns in our models.

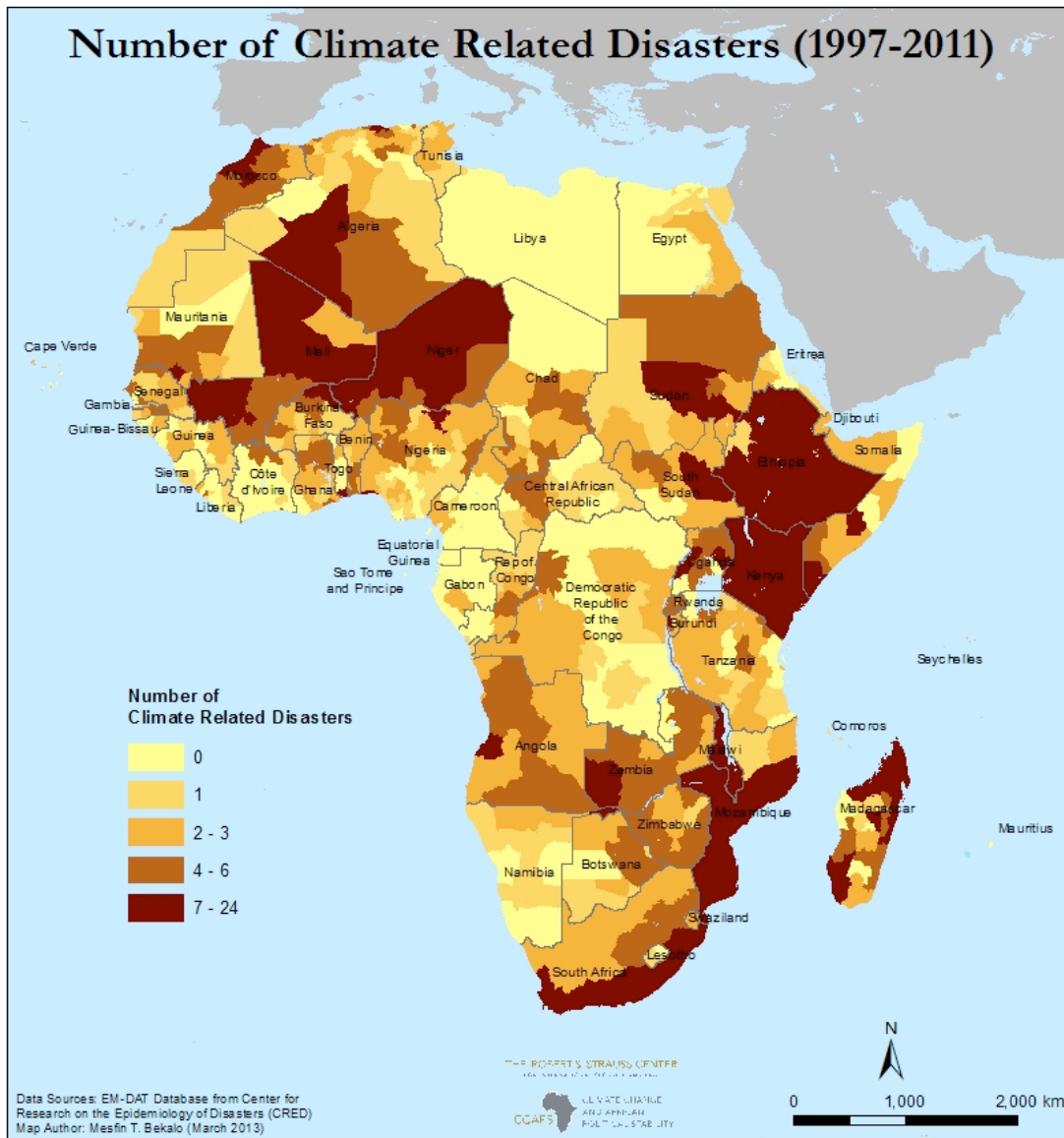
³² The criteria include: For a disaster to be entered into the database at least one of the following criteria must be fulfilled: ten (10) or more people reported killed, one hundred (100) or more people reported affected, a declaration of a state of emergency, or a call for international assistance. See <http://www.emdat.be/criteria-and-definition>

³³ This included droughts, floods, storms, wet landslides, wildfires, and extreme temperatures. Centre For Research on the Epidemiology of Disasters - CRED, “EM-DAT: The OFDA/CRED International Disaster Database”, 2011, www.emdat.net.

³⁴ Debarati Guha-Sapir, Jose M. Rodriguez-Llanes, and Thomas Jakubicka, “Using Disaster Footprints, Population Databases and GIS to Overcome Persistent Problems for Human Impact Assessment in Flood Events,” *Natural Hazards* 58, no. 3 (March 15, 2011): 845–852; P. Peduzzi and H. Dao C. Herold, “Mapping Disastrous Natural Hazards Using Global Datasets,” *Natural Hazards* 35, no. 2 (June 2005): 265–289.

³⁵ Special thanks to Madeline Clark for assisting with these efforts.

FIGURE 10: EM-DAT INCIDENCE OF DISASTER EVENTS



EM-DAT disaster events are concentrated in the Horn of Africa, the Sahel, and coastal Southern Africa. Of our four models, these patterns most closely resemble our additive Model 1 (Figure 6) and are population-weighted Model 3 (Figure 8), the two models with relatively wide geographic representation in our patterns of vulnerability. As in EM-DAT, areas in the Horn, Madagascar, coastal Mozambique, northern Nigeria, and

southern Niger correspond to high vulnerability areas in our model 1. At the same time, there are limits to a simple visual comparison. For one, areas of high disaster frequency in EM-DAT such as some regions in Kenya and South Africa are not reflected in our models.³⁶

Having said that, EM-DAT may not be more accurate than our portrait of vulnerability. Both Kenya and South Africa may possess more developed media and freedom of the press and thus exhibit reporting biases in the frequency of the press reports. Moreover, frequency counts do not capture the severity of different disaster events in terms of consequences. Most EM-DAT events have some geographic data specified and include some estimates of casualties, deaths, and damages. However, the consequences are not connected to individual locations where multiple towns or provinces are mentioned, making it difficult to know how to distribute the losses. Indeed, some of the first administrative divisions are quite large, and it is highly likely that attaching each event to the entire geographic area overstates the extent of the damage.

Given the vagueness of the geographic details in EM-DAT, connecting EM-DAT events to first administrative units is still better than nothing. In short, this exercise to compare our model findings to EM-DAT is a rough first cut and, to the extent that it reveals weaknesses in EM-DAT methods, perhaps it will serve to impel EM-DAT's organizers to develop a more robust geo-coding methodology.

Another possible external data source to validate our findings is the work by FEWS NET on food insecurity. They provided us with a map of West Africa to show areas that were "persistently" food insecure in the period July 2008 to April 2012, a

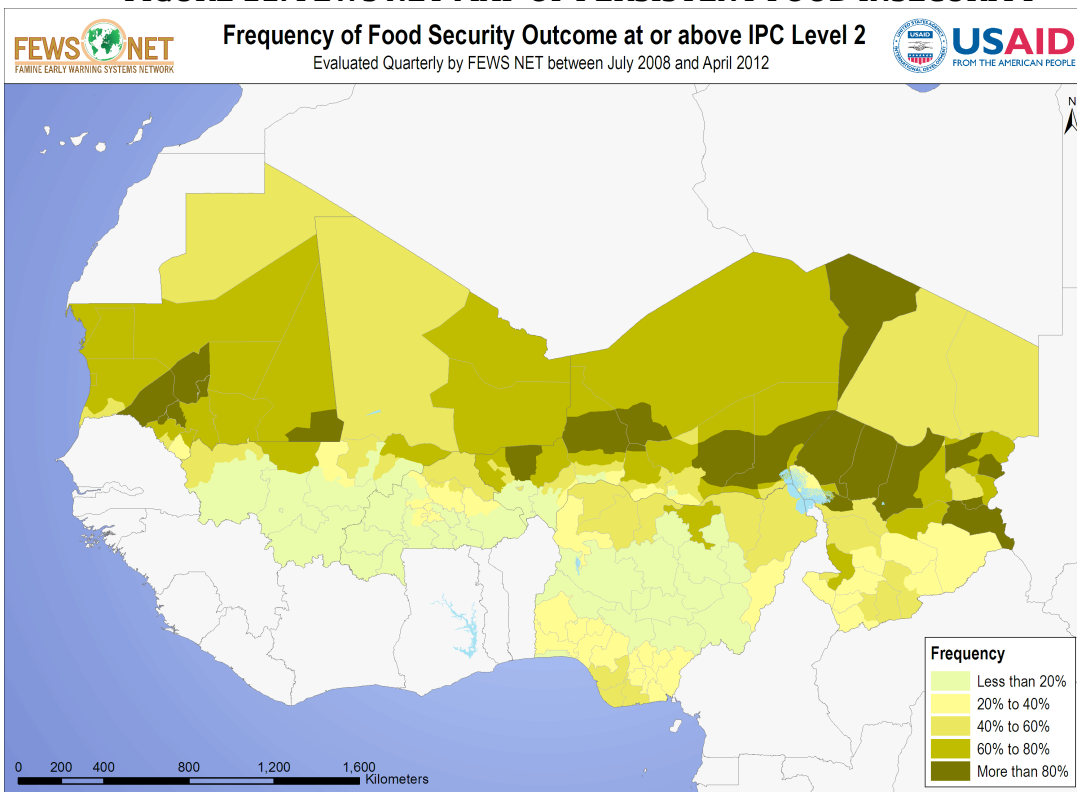
³⁶ These results are confirmed when one compares the mean resilience scores by administrative region with the number of EM-DAT events in that region or the percent rank of the number of events.

relatively short period but the best that FEWS NET could develop, given data availability (see Figure 11). Inputs in to the FEWS NET model include weather, climate, agriculture production, prices, trade, as well as an understanding of local livelihoods. The current scale for “acute food insecurity” consists of five phases including Phase 1 None/Minimal, Phase 2 Stressed, Phase 3 Crisis, Phase 4 Emergency, to Phase 5 Humanitarian Catastrophe/Famine. By the time you get to Phase 5, households face “near complete lack of food and/or other basic needs where starvation, death, and destitution are evident.”³⁷

One way to think about the map is as representing the “prevalence of food security.” Areas in light green reflect situations where less than 20% of the time, the area experienced “stressed” levels of food insecurity or higher. Thus, these areas (including southern Mali, southern Burkina Faso, parts of southwestern Niger, and central Nigeria) were relatively food secure and stable over this period. Dark green areas (namely the agro-pastoral band across the northern Sahel and southern Sahara) reflect situations where more than 80% of the time the location faced “stressed” levels of food insecurity or higher. In Figure 12, we zoom in to the same geographic area in our composite model 1 to see if the patterns are at all similar.

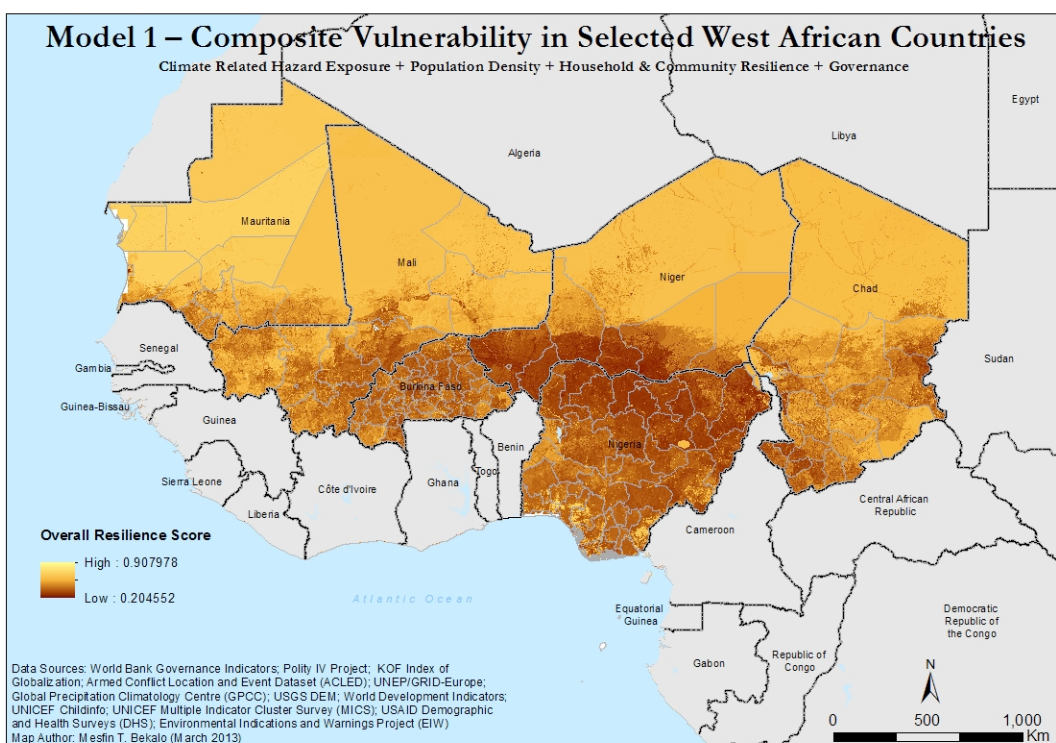
³⁷ The methodology for measuring food insecurity changed in April 2011 as USAID, the Food and Agricultural Organization, and a number of NGOs sought to standardize the methodology for measuring food insecurity through the new Integrated Food Security Phase Classification's (IPC) Acute Food Insecurity Reference Table for Household Groups. USAID FEWS NET, “IPC Acute Food Insecurity Reference Table for Household Groups,” Undated, <http://www.fews.net/ml/en/info/pages/scale.aspx>.

FIGURE 11: FEWS NET MAP OF PERSISTENT FOOD INSECURITY



Source: Famine Early Warning Systems Network (FEWS NET). Updated June 14, 2012. Based on quarterly Food Security Outcome analyses from October 2008 to April 2012.

FIGURE 12: CSVM 3.0 MODEL 1 OUTPUT



Based on these patterns, we see some superficial similarities in northern Nigeria and southern Niger, parts of Burkina Faso, and perhaps central Chad. It is less clear that our models show as much congruence over southern Nigeria and Chad. Moreover, the large northern regions of the lightly populated Sahel also appear more food insecure than our vulnerability maps depict because FEWS NET maps represent the percentage of the population at risk of food insecurity rather than the total number of people at risk.

It may be that we are attempting to compare too dissimilar concepts and metrics. FEWS NET maps are meant to capture some objective reality of areas that meet or exceed certain thresholds of food insecurity, whereas our maps are scaled to represent the relative vulnerability to climate security concerns of subnational areas of Africa in relation to the rest of the continent. While FEWS NET maps may ascribe high food insecurity to lightly populated areas, our maps would necessarily downplay the overall vulnerability in less densely populated regions.

One of the challenges FEWS NET faced in constructing their map is that the scale for measuring food insecurity changed over this period at least twice, with changes to the method, geographic units, and scale. FEWS NET maps are typically quarterly forecasts and the bias of earlier forecasts in the period may have been towards the more severe end of the spectrum. Beyond methodological changes to the rating scheme, the actual geographic units changed with political reorganizations so the map uses the most recent shape boundaries and reassigned values for the earlier periods based on the current units.

Still, these comparisons between our work and disasters, chronic food insecurity, and other climate related outcomes are important for us to assess the external validity of our models. Econometric work would also be a useful complement to the simple visual comparisons generated here.

Moreover, we should note that all three of these models depict historical outcomes rather than future consequences of climate change. As we have written about elsewhere, the future geographic distribution of the number and intensity of climate related hazards may be very different from the past.³⁸ For this reason, as we mentioned earlier, we have also collaborated with climate scientists on a mid 21st century regional climate projection for Africa to identify which regions historically vulnerable to climate related hazards are likely to face similar exposure in the future.

Conclusions

CSVM 3.0, our new maps of climate security vulnerability version 3.0, is a welcome advance over our previous methodology, benefiting from updated data sources, expanded subnational data, and a refined methodology for calculating and depicting vulnerability. Some areas, namely over the Horn of Africa, show persistent vulnerability across our models, both between and within iterations, and compare favorably with other data sources like EM-DAT. At the same time, we recognize that the stakes for getting this right are important, as resource allocation decisions for

³⁸ Joshua W. Busby et al., “Of Climate Change and Crystal Balls: The Future Consequences of Climate Change in Africa,” *Air & Space Power Journal Africa and Francophonie* no. 3 (2012): 4–44, http://www.airpower.au.af.mil/apjinternational/apj-af/2012/2012-3/eng/2012_3_05_Busby.pdf.

adaptation assistance may one day be related to estimates of the relative vulnerability of different regions. At the same time, we should recognize that these maps and the map-making process is an iterative conversation, meant to stimulate discussion about the priority areas in need of attention. The maps do not speak for themselves and are not the final word, requiring a more intense deliberation with regional experts. We look forward to that conversation.